# Co-binding of pharmaceutical compounds at mineral surfaces: mechanistic modeling of binding and co-binding of nalidixic acid and niflumic acid at goethite surfaces

Jing Xu [a,b], Rémi Marsac [b,c], Cheng Wei[b], Feng Wu [d], Jean-François Boily [e], Khalil Hanna [b]*

[a] State Key Laboratory of Water Resources and Hydropower Engineering Science, Wuhan University, Wuhan 430072, China.

[b]Ecole Nationale Supérieure de Chimie de Rennes, CNRS, UMR 6226, 11 Allée de Beaulieu, CS 50837, 35708 Rennes Cedex 7, France.

[c]Géosciences Rennes UMR 6118, Université Rennes 1, CNRS, 35042 Rennes cedex, France.

[d]Hubei Key Lab of Biomass Resource Chemistry and Environmental Biotechnology, School of Resources and Environmental Science, Wuhan University, Wuhan, 430079, P. R. China.

[e]Department of Chemistry, Umeå University, Umeå, SE-901 87, Sweden

*Corresponding author: ENSCR, Allée de Beaulieu, CS 50837, 35708 Rennes, France.

Tel.: +33 2 23 23 80 27, khalil.hanna@ensc-rennes.fr

A revised manuscript to *ES&T*

September, 2017

## Abstract

Although emerging contaminants rarely exist individually in environmental contaminated systems, only limited information on their adsorption mechanisms in multi-components solutions is currently available. To address this shortcoming, this work examines for the first time the accuracy of a surface complexation model in predicting the cooperative adsorption of nalidixic acid (NA) and niflumic acid (NFA) at goethite (α-FeOOH) surfaces. Our model adequately predicts co-binding of an outer-sphere (OS) complex of NFA onto NA bound to goethite through metal bonded (MB), hydrogen bonded (HB) or OS complexes. More positive charge is introduced in the system via sodium interactions in order to describe the NFA adsorption at high NaCl concentrations in both single and binary systems. Our model confidently predicts multilayers of NA on goethite as well as NFA binding on goethite-bound NA over a large range of pH, salinity as well as NA and NFA loadings. These findings have strong implications in the assessment and prediction of contaminant fate in multi-component contaminated systems by invoking a non-traditional form of ligand-ligand interaction in this field of study.

# Introduction

Although emerging contaminants (e.g. pharmaceutical and personal care products) often exist in mixture in environmental systems[1,2], they have been often studied individually with respect to the sorption and/or complexation with naturally occurring subsurface solids[3,4]. At environmental surfaces, the adsorption of multiple contaminants (or pollutant mixtures) can give way to competitive or cooperative binding. While competitive adsorption has been widely investigated[5–7], very few studies have resolved the impact of emerging contaminants co-binding at mineral surfaces. Very recently, we have demonstrated using vibrational spectroscopy and quantum chemical calculations[8], that nalidixic acid (NA, a quinolone antibiotic that is widely used in humans and animals medicine[9]) and niflumic acid (NFA, a non-steroidal anti-inflammatory that is often used for rheumatoid arthritis[2]) cooperatively adsorb to naturally-occurring mineral particles by intermolecular interactions (van der Waals). This novel finding raised the importance of recognizing drug co-binding as a mechanism contributing to the fate and transport of complex mixtures of antibiotics and anti-inflammatory agents in nature. Because most traditional environmental models are based on a single/individual contaminant basis, little is known on their fate in mixed contaminant systems. Omission of co-binding effects occurring in multi-component solutions might have unknown consequences on the prediction of fate and transport of these contaminants in the environment.

Some studies have used predictive models involving empirical adsorption isotherm equations with limited (site specific) applicability to describe the observed data in

multi-component solutions[10,11]. However, these macroscopic models cannot account for co-binding mechanisms for accurately predicting the behavior of antibiotics at mineral/water interfaces under a large range of physico-chemical conditions. In contrast, mechanistic models include details of the surface (in terms of structure), take into account the structure of the electrical interfacial layer[12–14], and constrain structure and bonding of surface complexes by information from spectroscopic studies and/or theoretical calculations[15–17]. Although mechanistic models have extensively been applied to predict pharmaceutical compounds adsorption to metal-(hydr)oxides[18,19], no attempt has been made to account for co-binding mechanisms between two or more components. This becomes even more important considering the necessity to adequately account for binding in reactive transport models to be used to predict the fate of antibiotics and anti-inflammatory agents in nature.

In this study, we used molecular-level information (Attenuated Total Reflectance-Fourier Transform InfraRed (ATR-FTIR) spectroscopy and quantum chemical calculations) obtained from our previous work[8], to develop a surface complexation model to account for the pH and salinity dependence of NA and NFA loadings achieved at goethite surfaces. We developed, for the first time, a model that accounts for co-binding of ligands resulting from van der Waals-type interactions. This opens new possibilities to account these generally overlooked forms of interactions in these types of studies in the future.

# 2. Materials and Methods

## 2.1. Chemicals

All chemicals used were of pro-analytical quality or better and were purchased from Sigma-Aldrich. Ultrapure water was used in all experiments. Goethite was prepared following Mazeina and Navrotsky's work[20]. Goethite (α-FeOOH) was selected due to its great thermodynamic stability, high surface reactivity with organic and inorganic ligands, and abundance in soils and sediments[21]. It has been characterized in detail in our previous work[8]. The specific surface area was of 81 ± 4 $m^2/g$ and the isoelectric point (IEP) is 9.1.

## 2.3. Batch experiments

The pH (3-10) and NaCl concentrations (3 – 300 mM) dependences of NA and NFA binding to goethite was first investigated in single ($[NA]_{tot}$ = 10 or 20 μM or $[NFA]_{tot}$ = 20 μM) and binary ($[NA]_{tot}$ = $[NFA]_{tot}$ = 20 μM) systems. pH adsorption edges in 10 mM NaCl and adsorption isotherms at pH 6 were taken from previous work[8], while pH-dependence of NA and NFA adsorption in single and binary systems at other NaCl concentrations (3, 100 and 300 mM) were conducted in the present work. Because high background electrolyte concentrations can affect pH measurements, the pH electrode was calibrated using solutions of known $[H^+]$ ($10^{-5}$–$10^{-3}$ M) at different [NaCl]. Therefore, pH refers to the molarity of the proton (−log $[H^+]$). Adsorption isotherms were obtained by experiments with (i) equimolar concentrations of NA and NFA (0.1 - 100 μM), (ii) varying concentrations of NFA (0.1 - 100 μM) with 20 μM

NA, and (iii) varying concentrations of NA (0.1 - 100 μM) with 20 μM NFA. Additionally, desorption tests conducted at pH = 11 were used to verify the mass balance of NA and NFA in the suspensions. They showed that solutes were removed only by adsorption, and that transformations by, for example, oxidation, did not occur under our experimental conditions (a result that is consistent with previous findings[22]).

Batch experiments were conducted in 10 mL suspensions of 0.5 g/L goethite in polypropylene tubes under an atmosphere of $N_2$(g) in order to avoid the effect of dissolved $CO_2$. Suspensions were mixed for a period of 8 h by end-over-end shaking, which is sufficient to reach a steady state[8]. Aliquots of the resulting suspensions were thereafter sampled and filtered (0.2 μm) for analysis. All adsorption experiments were performed at least twice, with a reproducibility of ~5% for NA- and ~10% for NFA-bearing systems.

Aqueous concentrations of NA and NFA were determined using high performance liquid chromatography (Waters 600 Controller) equipped with a photodiode array detector (Waters 996) and a reversed-phase C18 column (250 mm×4.6 mm i.d., 5 μm). The mobile phase (1 mL/min) was a mixture of acetonitrile/water (60/40 v/v) contained 0.1% formic acid. The detector was set to 258 nm for NA, 283 nm for NFA and both molecules could be analyzed with a single injection (NA: 4.5 min; NFA: 10.1 min).

### 2.4. Surface complexation modeling

The geochemical speciation code PHREEQC (version 2)[23] was used for surface

complexation calculations using thermodynamic database of Minteq. The $pK_a$s of NA ($pK_a$=6.19) and NFA ($pK_{a,1}$=2.28 and $pK_{a,2}$=5.10) at infinite dilution were obtained from conditional $pK_a$ values[24,25] and the Davies equation. NA exists as neutral (NAH, $pH < pK_a$) or anionic form ($NA^-$, $pH > pK_a$), and NFA as cationic ($NFAH_2^+$, $pH < pK_{a,1}$), anionic ($NFA^-$, $pH > pK_{a,2}$), neutral ($NFAH^0$) or zwiterionic form ($NFAH^{+/-}$) at $pK_{a,1} < pH < pK_{a,2}$. Molecular structures of the different dissolved NA and NFA species and calculated NA and NFA speciation versus pH in 10 mM NaCl solution are shown in Figure S1. Protonation reactions of NA and NFA are given in Table 1.

The charge of the goethite/water interface was treated with using the three plane model (TPM)[13], where charges of the adsorbates can be distributed between the 0- (metal-bonded complexes), 1- (hydrogen-bonded complexes), and 2-planes ($Na^+$, $Cl^-$, outer-sphere complexes). The TPM requires two capacitances for the 0- ($C_1$) and the 1-plane ($C_2$) which were taken from a previous study in our group[26]. Predictions of NA and NFA adsorption to goethite were made using the multi-site complexation (MUSIC) model [12]. For goethite, different types of surface sites can exist depending of the proportion of crystal planes, which should have different binding affinities. The goethite surface is considered to exhibit (101), (001) and (210) planes (group Pnma), which represent 63%, 27% and 10% of the total surface area, respectively. Singly ($\equiv FeOH^{-0.5}$), doubly ($\equiv Fe_2OH$) and triply ($\equiv Fe_3O^{-0.5}$ and $\equiv Fe_3OH^{+0.5}$) coordinated oxygens can be found at the goethite surface, depending on the crystal face. To simplify the model, we adopted the 1-pK approximation of the MUSIC model[12], neglecting the contributions of doubly- and part of the triply-coordinated oxygens. Crystallographic

153 site densities in this model are: [≡FeOH$^{-0.5}$]=3.03 sites/nm² at the (101), 3.34 sites/nm²
154 at the (001) and 7.4 sites/nm² at the (210) planes, and [≡$Fe_3O^{-0.5}$]=3.03 sites/nm² at the
155 (101) and 3.34 site/nm² at the (001) planes. The protonation constants of the groups are
156 set to that of the IEP (1-pK approach[14]). Formation constants of all surface species are
157 reported in Table 1.

158 NA and NFA are considered to bind only to ≡FeOH$^{-0.5}$ groups. From a molecular
159 viewpoint, ligands might also form H-bonds with doubly (≡$Fe_2$OH) and triply
160 (≡$Fe_3O^{-0.5}$ and ≡$Fe_3OH^{+0.5}$) coordinated sites. Recently, Boily[27] showed that
161 protonation of doubly-coordinated hydroxo groups and one type of triply-coordinated
162 oxo group, which are considered to be proton-silent within the 1-pK approach, may be
163 favored in the presence of strongly binding negatively charged ligand. However, a full
164 version of the MUSIC model for goethite would be required to account for all these
165 sites. This would lead to a drastic increase in the number of parameters and then
166 complexity in the model, and thus not considered in this modeling approach, as
167 generally carried out in literature[17–19,26,28–30].

168 The modeling strategy proceeded as follows. First, NA and NFA adsorption was
169 modeled in single systems. The corresponding surface complexation constants were
170 kept constant to model the NA-NFA binary system. All surface complexes reactions
171 involved in binding and co-binding mechanisms were proposed based on our own
172 molecular-level information and theoretical calculations and literature data, as detailed
173 below in section 3.

174 PhreePlot[31] was used to determine surface complexation constants and related

uncertainties for NA and NFA adsorption to goethite (single and binary systems). Charge variations at the 0-, 1- and 2-planes ($\Delta z_0$, $\Delta z_1$, $\Delta z_2$, respectively) are constrained by spatial considerations and are not adjustable parameters. PhreePlot contains an embedded version of the geochemical speciation program PHREEQC and it includes a parameter optimization procedure, which automatically fits a model to experimental data by minimizing the weighted sum of squares of the residuals. A modified Marquardt–Levenberg procedure was applied[32]. With this method, PhreePlot provides also a statistical uncertainty of the estimated parameters, which is given for each of optimized parameters in Table 1. Note that PHREEQC version 2 uses surface coverage fractions as standard state for surface species[33,34].

# 3. Results and discussion

**3.1. Nalidixic acid (NA) adsorption on goethite (single system).** As typically observed for many organic ligands, NA adsorption versus pH showed a bell-shape, and the maximum adsorption amount was observed at a pH near the p$K_a$ (Fig. 1a). Increasing NaCl concentration decreased NA adsorption on the whole investigated pH range ($[NA]_{tot}$ = 20 μM; Fig. 1), an effect that is generally attributed to non-specifically bound ligands at mineral surfaces[29,35].

According to the spectroscopic investigations of NA binding to goethite[8] and in agreement with previous studies on quinolone binding to minerals[29,36], MB surface complexes at the goethite (101)/(001) and (210) planes (Pnma group) were expected to

196 form *via* a NA keto group and one oxygen of the carboxylate group. This can be
197 expressed through the surface complexation reaction:

198

199 $2\ H^+ + 2\ \equiv FeOH^{-0.5} + NA^- \rightleftharpoons (\equiv Fe)_2(NA)^0 + 2\ H_2O \quad ; \quad \log\ ^{NA}K_{MB} \qquad (1)$

200

201 Only singly coordinated ($\equiv FeOH^{-0.5}$) surface sites were considered to be involved in the
202 latter reaction given the propensity for ligand exchange of these sites. Eq. 1 does not
203 denote the number of Fe(III) octahedra in a complex, but only the number of $\equiv FeOH^{-0.5}$
204 sites that may or may not be of the same Fe(III) octahedron[30]. Ideally, the steric
205 constraints at the dominant (101)/(001) planes (Pnma group) should promote bridging
206 between two Fe atoms separated by 3 Å from one another[37], while at the (210) plane,
207 two $\equiv FeOH^{-0.5}$ should be located on the same Fe(III) octahedron, hence our preference
208 for modeling NA binding as a 1:2 NA:$\equiv FeOH^{-0.5}$ species (Table 1).
209 Hydrogen-bonded (HB) complexation (surface hydration-shared ion pair) was
210 also modeled through singly $\equiv FeOH^{-0.5}$ sites with:[30]

211

212 $2\ H^+ + 2\ \equiv FeOH^{-0.5} + NA^- \rightleftharpoons (\equiv FeOH_2)_2^{+\cdots}(NA)^- \quad ; \quad \log\ ^{NA}K_{HB} \qquad (2)$

213

214 Formation of an outer-sphere (OS) complex (solvent-surface hydration-separated ion
215 pair), where NA keeps its first hydration sphere and its charge is located in the 2-plane,
216 was also considered to form with protonated singly-coordinated sites ($\equiv FeOH_2^{+0.5}$)
217 (Table 1).

As shown in Figure S2, our model satisfactorily predicts the pH dependence of NA adsorption to goethite at low NA loading ($[NA]_{tot} \leq 20$ μM; Fig. S2a,b,c), but underestimated the NA adsorption isotherm at pH 6 at high NA loadings (Fig. S2d). Furthermore, the effect of NaCl concentration on NA adsorption is not very well captured in this model, since this effect is small for $[NA]_{tot} = 10$ μM (Fig. S2a) but large for $[NA]_{tot} = 20$ μM (Fig. S2a,b). The corresponding highest adsorbed amount lies at 0.85 NA/nm² (i.e. 1.4 μmol/m²), and did not exceed the estimated NA loadings of ~1.5 NA/nm$^2$ that can be expected if all the ~ 3 –OH/nm$^2$ were to be consumed. Attempts to reproduce our data with the model of Boily[27] (i.e. using a full version of the MUSIC model for goethite including more surface sites for HB and OS complexes) led to similar conclusions (not shown). We thus conclude that calculated NA adsorption amount at high loading is not limited by the number of available surface sites, but by less favorable electrostatic effects due to surface charge neutralization by NA.

In fact, higher loadings favor additional binding mechanisms (e.g. multilayer, dimerization, hydrophobic interactions and surface precipitation) involving direct NA-NA interactions. Drawing from our previous work on intermolecular interactions between naphthoic acids[16], we can write:

$$2\ H^+ + 2\ \equiv FeOH^{-0.5} + 2\ NA^- \rightleftharpoons (\equiv Fe)_2NA^{0\cdots}(NA)^- + 2\ H_2O\ ;\quad \log\ {}^{NA}K_{dimer} \qquad (3)$$

In this equation, a NA-NA dimer is formed by co-bonding to individual NA molecules, resulting in an interfacial distribution of charges between the 0- and 1-planes.

Combining the equations with monomer and dimer of NA, the model better predicts NA adsorption at high loadings (Fig. 1d).

In summary, surface complexation modeling results (Table 1, Fig. 1 and Fig. S3), predict NA binding as a function of pH (Fig. 1a and Fig. S3 for $[NA]_{tot}$ = 20 and 10 μM, respectively), NaCl concentration (Fig. 1 a,c) and NA loadings (Fig. 1d). In accordance with previous reports on ligand binding (e.g. for benzenecarboxylates[30]), NA predominantly formed HB and OS complexes at high pH while MB complexes only formed at pH < 7 (Fig. 1a). The model also predicts NA dimer formation with NA between pH 3 and 7 (Fig. 1 a,d).

**3.2. Niflumic acid (NFA) adsorption on goethite (single system).** NFA binding followed the same pH dependence as NA (Fig. 1b) but is favored at NaCl concentration greater than 50 mM (Fig. 1c). This alongside the weaker dependence of binding on NFA loadings (Fig. 1d) suggests distinct binding mechanisms to those of NA. In fact, based on the disposition of its functional groups, HB and OS complexation should predominate over MB species under all conditions considered in this work, as for example for other monocarboxylate ligands such as acetate, benzoate, cyclohexanecarboxylate or naphthoate[17,35]. Both HB and OS complexes were expressed by the following reaction:

$$2\,H^+ + 2\,{\equiv}FeOH^{-0.5} + NFA^- \rightleftharpoons ({\equiv}FeOH_2)_2^{+\cdots}NFA^- \quad ; \log {}^{NFA}K_{HB/OS} \quad (4)$$

here omitting the intervening roles of water. The -1 charge of the HB complex of NFA is located at the 1-plane ($\Delta z_1 = -1$; $\Delta z_2 = 0$) whereas that of the OS complex is in the 2-plane ($\Delta z_1 = 0$; $\Delta z_2 = -1$). This model adequately accounts for all goethite-NFA data, except the effect of NaCl concentration. Alternatively, replacing the HB complex with its zwitterion form provides both an adequate prediction of binding with pH and NaCl concentration below pH 6, and is consistent with previous accounts[18,19,38] supporting this type of species.

$$3\ H^+ + 2\ \equiv FeOH^{-0.5} + NFA^- \rightleftharpoons (\equiv FeOH_2)_2^{+\cdots}NFAH^0 \quad ; \log {}^{NFA}K_{HBH} \qquad (5)$$

Preliminary calculations showed that HB complexes with anionic or zwitterionic form of NFA occurred in a comparable pH-range (not shown). To simplify the model, the HB complex with the anionic form was removed from the speciation scheme. The OS species is however needed to account for the high pH data at NaCl concentrations below 10 mM. This model accurately predicts NFA adsorption at 10 mM NaCl but provides a poor description of NaCl effect (Fig. S4). Because of the increasing adsorption of NFA at high NaCl concentration, a sodium-OS ion pair is however needed to account for the data above 10 mM NaCl through:

$$2\ H^+ + 2\ \equiv FeOH^{-0.5} + NFA^- + Na^+ \rightleftharpoons (\equiv FeOH_2)_2^{+\cdots}NFA^{-\cdots}Na^+ \quad ; \log {}^{NFA}K_{HBNa} \qquad (6)$$

where $Na^+$ charge is located in the 2-plane. Sodium co-binding has been previously proposed to describe the adsorption of phosphate to goethite[39]. This model allows a relatively good prediction of NFA adsorption to goethite at various pH (Fig. 1b), [NaCl] (Fig. 1b,c) and [NFA] (Fig. 1d).

### 3.3. Binary NA-NFA system

NA-NFA co-binding occurred over a large range of pH (Fig. 2a,b), NaCl concentrations (Fig. 2a,b,e) and NA and NFA loadings (Fig. 2c,d). Co-binding effect is more pronounced for NFA, because of its weaker adsorption in single system. However, NA adsorption to goethite is rather strong in single system, and so co-binding with NFA only further stabilizes NA at the surface. As a result, to accurately predict binding in mixed NA-NFA system, the model requires reactions accounting of cooperative effects between NA and NFA besides the competitive binding mechanisms of eqs. 1-6. This is further illustrated in Figure S5, where NA and NFA adsorption in binary system is strongly underestimated when using only eqs. 1-6.

For NA, all MB, HB and OS complexes of NA are considered to be formed because of the similar shape of the adsorption edges in mixtures with those of the single system (Figs. 1a and 2a), while only OS complexes are considered for NFA because the maximal loadings of NFA (Fig. 2b) coincided with that achieved in the single system (Fig. 1b). To keep the model at a reasonable level of complexity we however only considered the binary NA-NFA surface complex at the (101)/(001) planes and model co-binding with:

$$2\ H^+ + 2\ \equiv FeOH^{-0.5} + NA^- + NFA^- \rightleftharpoons$$

$$(\equiv Fe)_2(NA)^{0\cdots}(NFA)^- + 2\ H_2O \quad ; \quad \log K_{MB\text{-}OS} \qquad (7)$$

$$2\ H^+ + 2\ \equiv FeOH^{-0.5} + NA^- + NFA^- \rightleftharpoons$$

$$(\equiv FeOH_2)_2^{+\cdots-}(NA)\ \cdots\ (NFA)^- \quad ; \quad \log K_{HB\text{-}OS} \qquad (8)$$

$$2\ H^+ + 2\ \equiv FeOH^{-0.5} + NA^- + NFA^- \rightleftharpoons$$

$$(\equiv FeOH_2)_2^{+\cdots-}(NA)\ \cdots\ (NFA)^- \quad ; \quad \log K_{OS\text{-}OS} \qquad (9)$$

In eq. 7-9, NFA binds to one NA at the goethite surface predominantly via van der Waals interactions[8], and its -1 charge is located at the 2-plane. In contrast, NA is assumed to form MB, HB and OS complexes with goethite, respectively, and its -1 charge should therefore be located at the 0-plane ($\Delta z_0$=+1; $\Delta z_1$=0; $\Delta z_2$=-1, eq. 7), the 1-plane ($\Delta z_0$=+2; $\Delta z_1$=-1; $\Delta z_2$=-1, eq. 8) or the 2-plane ($\Delta z_0$=+2; $\Delta z_1$=0; $\Delta z_2$=-2, eq. 9). Note that the reverse case (NA binding to adsorbed NFA) involves the same stoichiometry and charge distribution over the 0-, 1- and 2-planes. Therefore, they are equivalent in PHREEQC. However, previous quantum chemical calculations[8] suggested that the reverse case was less plausible, that is, NA was expected to be located closer than NFA to the surface.

Our first modeling attempts using eqns. 1-9 predicted a decrease of NA/NFA adsorption with increasing [NaCl], which is inconsistent with experimental

observations (see Figure S6). Most notably, experimental NA binding became almost independent of NaCl concentration (Fig. 2a,e) while NFA binding followed three stages: (i) slight decrease in loadings below 10 mM, (ii) increased loadings at 10-50 mM, and (iii) constant loadings above 50 mM NaCl (Fig. 2b,e). Including of an ion pair with sodium

$$2\,H^{+} + 2\,{\equiv}FeOH^{-0.5} + NA^{-} + NFA^{-} + Na^{+} \rightleftharpoons$$

$$({\equiv}FeOH_2)_2^{+\cdots-}(NA)\cdots(NFA)^{-}\cdots Na^{+} \quad ; \quad \log K_{HB\text{-}HB\text{-}Na} \qquad (10)$$

considerably improved model predictions of the effect of NaCl (Fig. 2a,b,e). The best fit was obtained by allocating charges of both NA and NFA in the 1-plane and $Na^{+}$ in the 2-plane ($\Delta z_0$=+2; $\Delta z_1$=-2; $\Delta z_2$=+1) (Table 1).

The full model (i.e. eqs.1-10) provides an accurate description of co-binding data *vs* pH and NaCl concentration (Fig. 2a, b) and at a wide range of aqueous concentration (0.1- 100 µM) (Fig. 2c). This also permits to fit very well the variation of $[NFA]_{ads}$ as a function of $[NA]_{ads}$ regardless of the adopted approach : (i) varying $[NA]_{tot}$ at constant $[NFA]_{tot}$, (ii) varying $[NFA]_{tot}$ at constant $[NA]_{tot}$ or (iii) varying equimolar concentration of both (Fig. 2d).

Model predictions of NA and NFA surface speciation for 10 mM NaCl (Figs. 2 a,b) suggest that NA-NFA dimers remarkably prevail at pH > 4. Although NA adsorption slightly increased from the single to the binary system, its surface speciation drastically changes, probably due to competition between the three forms of NA (NA monomer,

NA dimer and NA-NFA dimer). Indeed, proportions of monomeric and dimeric forms of NA strongly diminished in favor of NA-NFA surface complexes (Fig. 2a, c). NFA adsorption was, however, mainly dominated by the formation of NA-NFA surface complexes (Fig. 2b, c).

Finally, our proposed model not only explains batch adsorption data generated for this work but also concentration profiles of dominant species extracted by a chemometric analysis[40] of our previously published[8] Fourier Transform Infrared spectra on these systems (Fig. 2f). Our work had shown that vibration spectra of mixed NA+NFA+goethite could not be explained as a linear combination of isolated NA+goethite and NFA+goethite systems. The concentration profiles in Fig. 2f show that increasing fractions of NA-NFA complexed with increasing $[NA]_{tot}$ (constant $[NFA]_{tot}$) or with increasing $[NFA]_{tot}$ ($[NA]_{tot}$) are well-predicted by the model. This adds further confidence to the ability of our proposed model to account for NA and NFA binding in single and mixed systems.

**Implications for reactive transport modeling.** Because of the increase of multiple contaminations in aquatic ecosystems worldwide, environmental subsurface and groundwaters often contain multiple contaminants including nonprescription drugs, antibiotics, hormones and prescription drugs[41]. Protection of groundwater resources requires an accurate assessment of processes controlling the contaminant fate and transport in complex environmental mixtures.

The development of new surface complexation models to account for co-binding at

mineral surfaces is central to the prediction of the fate of contaminants in multi-component systems. We demonstrate, for the first time, that co-binding of emerging organic contaminants (e.g. NA and NFA) can be predicted over a large range of environmentally relevant conditions using a mechanistic model based on insights from vibration spectroscopy and quantum chemical calculations[8]. The modeling approach accounting for new forms of drugs co-binding at mineral surfaces is becoming a powerful tool for implementation of co-binding phenomena in reactive transport models, and for the accurate prediction of the transport of antibiotics and anti-inflammatory agents in soils and sediments.

**Acknowledgements**

This work was supported by Rennes Métropole (AIS 2013 to K.H.) and by the Swedish Research Council (2016-03808 to J.-F.B.). We also gratefully acknowledge the CNRS-NSFC PRC common grant (CNRS No. 270437 and NSFC-CNRS_PRC No. 21711530144) for providing financial support.

**Supporting information available**

NA and NFA aqueous speciation versus pH and additional modeling tests. This information is available free of charge via the Internet at http://pubs.acs.org/.

391 **References**

392

393 (1) Gothwal, R.; Shashidhar, T. Antibiotic Pollution in the Environment: A Review.
394 *CLEAN--Soil, Air, Water* **2015**, *43* (4), 479–489.
395 (2) Fatta-Kassinos, D.; Meric, S.; Nikolaou, A. Pharmaceutical residues in
396 environmental waters and wastewater: Current state of knowledge and future
397 research. *Anal. Bioanal. Chem.* **2011**, *399* (1), 251–275.
398 (3) Xu, X.-R.; Li, X.-Y. Sorption and desorption of antibiotic tetracycline on marine
399 sediments. *Chemosphere* **2010**, *78* (4), 430–436.
400 (4) Kulshrestha, P.; Giese, R. F.; Aga, D. S. Investigating the molecular interactions
401 of oxytetracycline in clay and organic matter: insights on factors affecting its
402 mobility in soil. *Environ. Sci. Technol.* **2004**, *38* (15), 4097–4105.
403 (5) Hiemstra, T.; Van Riemsdijk WH. Surface Structural Ion Adsorption Modeling
404 of Competitive Binding of Oxyanions by Metal (Hydr)oxides. *J. Colloid*
405 *Interface Sci.* **1999**, *210* (1), 182–193.
406 (6) Conkle, J. L.; Lattao, C.; White, J. R.; Cook, R. L. Competitive sorption and
407 desorption behavior for three fluoroquinolone antibiotics in a wastewater
408 treatment wetland soil. *Chemosphere* **2010**, *80* (11), 1353–1359.
409 (7) Xing, B.; Pignatello, J. J. Competitive sorption between 1, 3-dichlorobenzene or
410 2, 4-dichlorophenol and natural aromatic acids in soil organic matter. *Environ.*
411 *Sci. Technol.* **1998**, *32* (5), 614–619.
412 (8) Xu, J.; Marsac, R.; Costa, D.; Cheng, W.; Wu, F.; Boily, J. F.; Hanna, K.

Co-Binding of Pharmaceutical Compounds at Mineral Surfaces: Molecular Investigations of Dimer Formation at Goethite/Water Interfaces. *Environ. Sci. Technol.* **2017**, *51* (15), 8343–8349.

(9) Zhang, T.; Li, B. Occurrence, Transformation, and Fate of Antibiotics in Municipal Wastewater Treatment Plants. *Crit. Rev. Environ. Sci. Technol.* **2011**, *41* (11), 951–998.

(10) Limousin, G.; Gaudet, J. P.; Charlet, L.; Szenknect, S.; Barthès, V.; Krimissa, M. Sorption isotherms: A review on physical bases, modeling and measurement. *Appl. Geochemistry* **2007**, *22* (2), 249–275.

(11) Liu, S. Cooperative adsorption on solid surfaces. *J. Colloid Interface Sci.* **2015**, *450*, 224–238.

(12) Hiemstra, T.; Van Riemsdijk, W. H. A surface structural approach to ion adsorption: the charge distribution (CD) model. *J. Colloid Interface Sci.* **1996**, *179* (2), 488–508.

(13) Filius, J. D.; Hiemstra, T.; Van Riemsdijk, W. H. Adsorption of Small Weak Organic Acids on Goethite: Modeling of Mechanisms. *J. Colloid Interface Sci.* **1997**, *195* (2), 368–380.

(14) Gaboriaud, F.; Ehrhardt, J. J. Effects of different crystal faces on the surface charge of colloidal goethite (α-FeOOH) particles: An experimental and modeling study. *Geochim. Cosmochim. Acta* **2003**, *67* (5), 967–983.

(15) Hiemstra, T.; Barnett, M. O.; van Riemsdijk, W. H. Interaction of silicic acid with goethite. *J. Colloid Interface Sci.* **2007**, *310* (1), 8–17.

435 (16) Boily, J. F.; Sjöberg, S.; Persson, P. Structures and stabilities of Cd(II) and
436 Cd(II)-phthalate complexes at the goethite/water interface. *Geochim.*
437 *Cosmochim. Acta* **2005**, *69* (13), 3219–3235.
438 (17) Hanna, K.; Boily, J.-F. Sorption of two naphthoic acids to goethite surface under
439 flow through conditions. *Environ. Sci. Technol.* **2010**, *44* (23), 8863–8869.
440 (18) Paul, T.; Machesky, M. L.; Strathmann, T. J. Surface complexation of the
441 zwitterionic fluoroquinolone antibiotic ofloxacin to nano-anatase TiO2
442 photocatalyst surfaces. *Environ. Sci. Technol.* **2012**, *46* (21), 11896–11904.
443 (19) Paul, T.; Liu, J.; Machesky, M. L.; Strathmann, T. J. Adsorption of zwitterionic
444 fluoroquinolone antibacterials to goethite: A charge distribution-multisite
445 complexation model. *J. Colloid Interface Sci.* **2014**, *428*, 63–72.
446 (20) Mazeina, L.; Navrotsky, A. Surface Enthalpy of Goethite. *Clays Clay Miner.*
447 **2005**, *53* (2), 113–122.
448 (21) Schwertmann, U.; Taylor, R. M. Iron oxides. Pp. 379-438 in: Minerals in Soil
449 Environments (JB Dixon and SB Weed, editors). *Soil Sci. Soc. Am. Madison,*
450 *Wisconsin, USA* **1989**.
451 (22) Clervil, E.; Usman, M.; Emmanuel, E.; Chatain, V.; Hanna, K. Sorption of
452 nalidixic acid onto sediments under batch and dynamic flow conditions. *Chem.*
453 *Geol.* **2013**, *335*, 63–74.
454 (23) Parkhurst, D. L.; Appelo, C. A. J.; others. User's guide to PHREEQC (Version
455 2): A computer program for speciation, batch-reaction, one-dimensional
456 transport, and inverse geochemical calculations. **1999**.

(24) Ross, D. L.; Riley, C. M. Aqueous solubilities of some variously substituted quinolone antimicrobials. *Int. J. Pharm.* **1990**, *63* (3), 237–250.

(25) Takács-Novák, K.; Tam, K. Y. Multiwavelength spectrophotometric determination of acid dissociation constants: Part V: microconstants and tautomeric ratios of diprotic amphoteric drugs. *J. Pharm. Biomed. Anal.* **2000**, *21* (6), 1171–1182.

(26) Hanna, K.; Martin, S.; Quilès, F.; Boily, J.-F. Sorption of Phthalic Acid at Goethite Surfaces under Flow-Through Conditions. *Langmuir* **2014**, *30* (23), 6800–6807.

(27) Boily, J.-F. Water structure and hydrogen bonding at goethite/water interfaces: Implications for proton affinities. *J. Phys. Chem. C* **2012**, *116* (7), 4714–4724.

(28) Venema, P.; Hiemstra, T.; van Riemsdijk, W. H. Multisite adsorption of cadmium on goethite. *J. Colloid Interface Sci.* **1996**, *183* (2), 515–527.

(29) Marsac, R.; Martin, S.; Boily, J.-F.; Hanna, K. Oxolinic acid binding at goethite and akaganéite surfaces: implications for aquaculture-induced pollution. *Environ. Sci. Technol.* **2016**, *50* (2), 660–668.

(30) Boily, J.-F.; Persson, P.; Sjöberg, S. Benzenecarboxylate surface complexation at the goethite (α-FeOOH)/water interface: II. Linking IR spectroscopic observations to mechanistic surface complexation models for phthalate, trimellitate, and pyromellitate. *Geochim. Cosmochim. Acta* **2000**, *64* (20), 3453–3470.

(31) Kinniburgh, D.; Cooper, D. PhreePlot: Creating graphical output with

PHREEQC. http://www.phreeplot.org. **2011**.

(32) Powell, M. J. D. A Method for Minimizing a Sum of Squares of Non-Linear Functions Without Calculating Derivatives. *Comput. J.* **1965**, *7* (1), 303–307.

(33) Lützenkirchen, J.; Marsac, R.; Kulik, D. A.; Payne, T. E.; Xue, Z.; Orsetti, S.; Haderlein, S. B. Treatment of multi-dentate surface complexes and diffuse layer implementation in various speciation codes. *Appl. Geochemistry* **2015**, *55*, 128–137.

(34) Wang, Z. M.; Giammar, D. E. Mass Action Expressions for Bidentate Adsorption in Surface Complexation Modeling: Theory and Practice. *Environ. Sci. Technol.* **2013**, *47* (9), 3982–3996.

(35) Norén, K.; Persson, P. Adsorption of monocarboxylates at the water/goethite interface: The importance of hydrogen bonding. *Geochim. Cosmochim. Acta* **2007**, *71* (23), 5717–5730.

(36) Gu, C.; Karthikeyan, K. G. Sorption of the antimicrobial ciprofloxacin to aluminum and iron hydrous oxides. *Environ. Sci. Technol.* **2005**, *39* (23), 9166–9173.

(37) Boily, J. F.; Kozin, P. A. Particle morphological and roughness controls on mineral surface charge development. *Geochim. Cosmochim. Acta* **2014**, *141*, 567–578.

(38) Gu, X.; Tan, Y.; Tong, F.; Gu, C. Surface complexation modeling of coadsorption of antibiotic ciprofloxacin and Cu (II) and onto goethite surfaces. *Chem. Eng. J.* **2015**, *269*, 113–120.

(39) Rahnemaie, R.; Hiemstra, T.; Van Riemsdijk, W. H. Geometry, charge distribution, and surface speciation of phosphate on goethite. *Langmuir* **2007**, *23* (7), 3680–3689.

(40) Jaumot, J.; Gargallo, R.; de Juan, A.; Tauler, R. A graphical user-friendly interface for MCR-ALS: a new tool for multivariate curve resolution in MATLAB. *Chemom. Intell. Lab. Syst.* **2005**, *76* (1), 101–110.

(41) Schwarzenbach, R. P.; Escher, B. I.; Fenner, K.; Hofstetter, T. B.; Johnson, C. A.; von Gunten, U.; Wehrli, B. The challenge of micropollutants in aquatic systems. *Science* **2006**, *313* (5790), 1072–1077.

512 **Table 1. Model parameters.**

| | Complex | log K | $\Delta z_0$ | $\Delta z_1$ | $\Delta z_2$ |
|---|---|---|---|---|---|
| $NA^- + H^+ = NAH$ | | 6.19 | | | |
| $NFA^- + H^+ = NFAH$ | | 5.10 | | | |
| $NFAH + H^+ = NFAH_2^+$ | | 2.28 | | | |
| $\equiv Fe_3O^{-0.5} + H^+ \rightleftharpoons \equiv Fe_3OH^{+0.5}$ | | 9.1 | +1 | 0 | 0 |
| $\equiv Fe_3O^{-0.5} + H^+ + Cl^- \rightleftharpoons \equiv Fe_3OH_2^{+0.5}\cdots Cl^-$ | | 8.1 | +1 | 0 | -1 |
| $\equiv Fe_3O^{-0.5} + Na^+ \rightleftharpoons \equiv Fe_3OH^{-0.5}\cdots Na^+$ | | -1 | 0 | 0 | +1 |
| $\equiv FeOH^{-0.5} + H^+ \rightleftharpoons \equiv FeOH_2^{+0.5}$ | | 9.1 | +1 | 0 | 0 |
| $\equiv FeOH^{-0.5} + H^+ + Cl^- \rightleftharpoons \equiv FeOH_2^{+0.5}\cdots Cl^-$ | | 8.1 | +1 | 0 | -1 |
| $\equiv FeOH^{-0.5} + Na^+ \rightleftharpoons \equiv FeOH^{-0.5}\cdots Na^+$ | | -1 | 0 | 0 | +1 |
| $2\ H^+ + 2 \equiv FeOH^{-0.5} + NA^- \rightleftharpoons (\equiv Fe)_2(NA)^0 + 2\ H_2O$ | MB | 19.7±0.1 | +1 | 0 | 0 |
| $2\ H^+ + 2 \equiv FeOH^{-0.5} + NA^- \rightleftharpoons (\equiv FeOH_2)_2^+\cdots NA^-$ | HB | 20.0±0.1 | +2 | -1 | 0 |
| $2\ H^+ + 2 \equiv FeOH^{-0.5} + NA^- \rightleftharpoons (\equiv FeOH_2)_2^+\cdots NA^-$ | OS | 20.8±0.1 | +2 | 0 | -1 |
| $2\ H^+ + 2 \equiv FeOH^{-0.5} + 2\ NA^- \rightleftharpoons (\equiv Fe)_2(NA)^0\cdots NA^-$ | dimer | 22.2±0.1 | +1 | -1 | 0 |
| $3\ H^+ + 2 \equiv FeOH^{-0.5} + NFA^- \rightleftharpoons (\equiv FeOH_2)_2^+\cdots NFAH$ | HBH | 27.0±0.1 | +2 | 0 | 0 |
| $2\ H^+ + 2 \equiv FeOH^{-0.5} + NFA^- \rightleftharpoons (\equiv FeOH_2)_2^+\cdots NFA^-$ | OS | 19.9±0.1 | +2 | 0 | -1 |
| $2\ H^+ + 2 \equiv FeOH^{-0.5} + NFA^- + Na^+ \rightleftharpoons (\equiv FeOH_2)_2^+\cdots NFA^-\cdots Na^+$ | HB-Na | 20.8±0.1 | +2 | -1 | +1 |
| $2\ H^+ + 2 \equiv FeOH^{-0.5} + NA^- + NFA^- \rightleftharpoons (\equiv Fe)_2(NA)^0\cdots NFA^-$ | MB-OS | 23.2±0.2 | +1 | 0 | -1 |
| $2\ H^+ + 2 \equiv FeOH^{-0.5} + NA^- + NFA^- \rightleftharpoons (\equiv FeOH_2)_2^+\cdots NA^-\cdots NFA^-$ | HB-OS | 23.2±0.2 | +2 | -1 | -1 |
| $2\ H^+ + 2 \equiv FeOH^{-0.5} + NA^- + NFA^- \rightleftharpoons (\equiv FeOH_2)_2^+\cdots NA^-\cdots NFA^-$ | OS-OS | 25.4±0.2 | +2 | 0 | -2 |
| $2\ H^+ + 2 \equiv FeOH^{-0.5} + NA^- + NFA^- + Na^+ \rightleftharpoons (\equiv FeOH_2)_2^+\cdots NA\text{-}NFA^{2-}\cdots Na^+$ | HB-HB-Na | 26.3±0.2 | +2 | -2 | +1 |

513

514 TPM with $C_1$=2.3 F/m², $C_2$=1.07 F/m²; 63% of (101), 27% of (001) and 10% of (210). Site
515 densities: $[\equiv FeOH^{-0.5}]$=3.03, 3.34 and 7.4 site/nm² at the (101), (001) and (210) planes,
516 respectively; $[\equiv Fe_3O^{-0.5}]$=3.03 and 3.34 site/nm² at the (101) and (001) planes, respectively. HB,
517 OS and binary NA-NFA complexes are considered to form at all planes ((101)/(001)/(210)). NA
518 and NFA surface complexation constants and uncertainty obtained with Phreeplot. All other
519 parameters were fixed.
520

## Figure captions

**Figure 1.** Single systems. Adsorption of 20 μM (a) NA and (b) NFA to goethite (0.5 g/L) versus pH and [NaCl] (3-100 mM). (c) Adsorption of 20 μM NA or NFA (20 μM) on goethite (0.5 g/L) versus [NaCl] at pH 5. (d) NA-goethite and NFA-goethite adsorption isotherms at pH 6 in 10 mM NaCl, where NA surface speciation is shown ("total" refers to overall modeled adsorption results). In all graphs, full lines correspond to overall adsorption predicted by surface complexation modeling. In (a) and (b) NA and NFA surface speciation is shown as discontinuous lines (for 10 mM NaCl). MB, HB and OS denote metal-bonded, hydrogen-bonded and outer-sphere complexes, respectively.

**Figure 2.** Binary NA-NFA system. Adsorption of (a) NA and (b) NFA to goethite (0.5 g/L) versus pH and [NaCl] (3-300 mM) for $[NA]_{tot} = [NFA]_{tot} = 20$ μM. (c) NA and NFA adsorption isotherms at pH 6 in 10 mM NaCl for $[NA]_{tot} = [NFA]_{tot}$. (d) $[NFA]_{ads}$ vs $[NA]_{ads}$ for three experimental conditions: (i) ($[NFA]_{tot} = 20$ μM, varying $[NA]_{tot}$, black), (ii) ($[NA]_{tot} = 20$ μM, varying $[NFA]_{tot}$, red), and (iii) varying both compounds with $[NA]_{tot} = [NFA]_{tot}$ (blue). (e) Adsorption of NA and NFA ($[NA]_{tot} = [NFA]_{tot} = 20$ μM) on goethite (0.5 g/L) versus [NaCl] at pH 5. In all graphs, full lines correspond to overall adsorption predicted by surface complexation modeling (using the same color as the corresponding symbol). In (a), (b) and (c) NA and NFA surface speciation is shown as discontinuous lines (for 10 mM NaCl). "total" refers to overall modeled adsorption results in (c). (f) Concentration profiles extracted by chemometric modeling of FTIR data[8] for the series corresponding to constant $[NA]_{tot}$ and varying $[NFA]_{tot}$ (black) or constant $[NFA]_{tot}$ and varying $[NA]_{tot}$ (red).

554

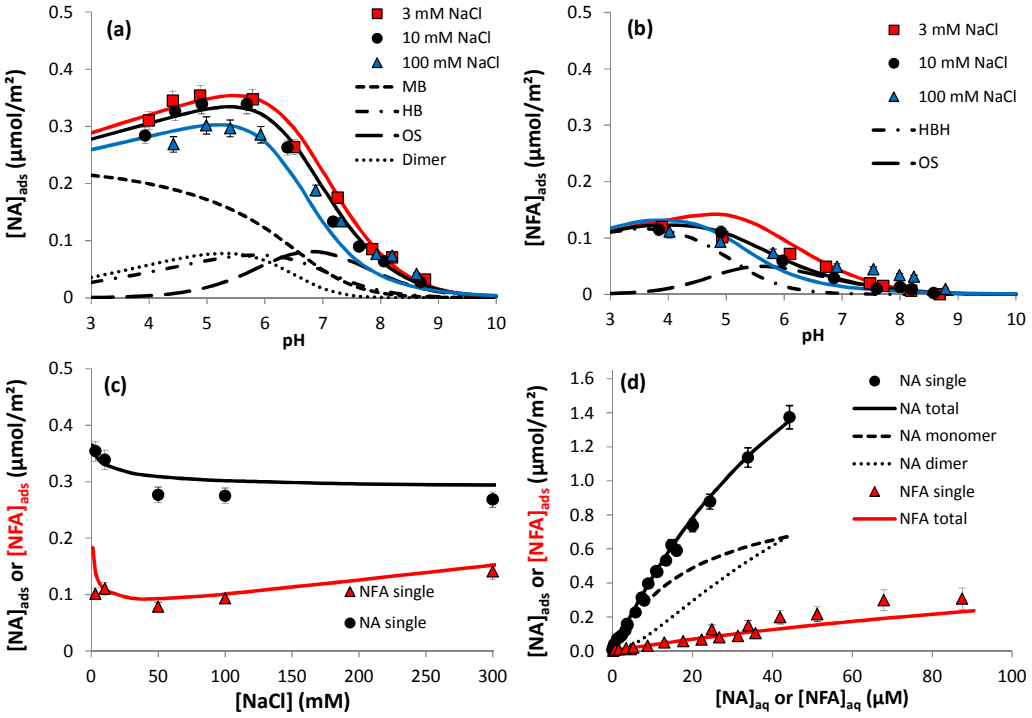


555

556 **Figure 1**

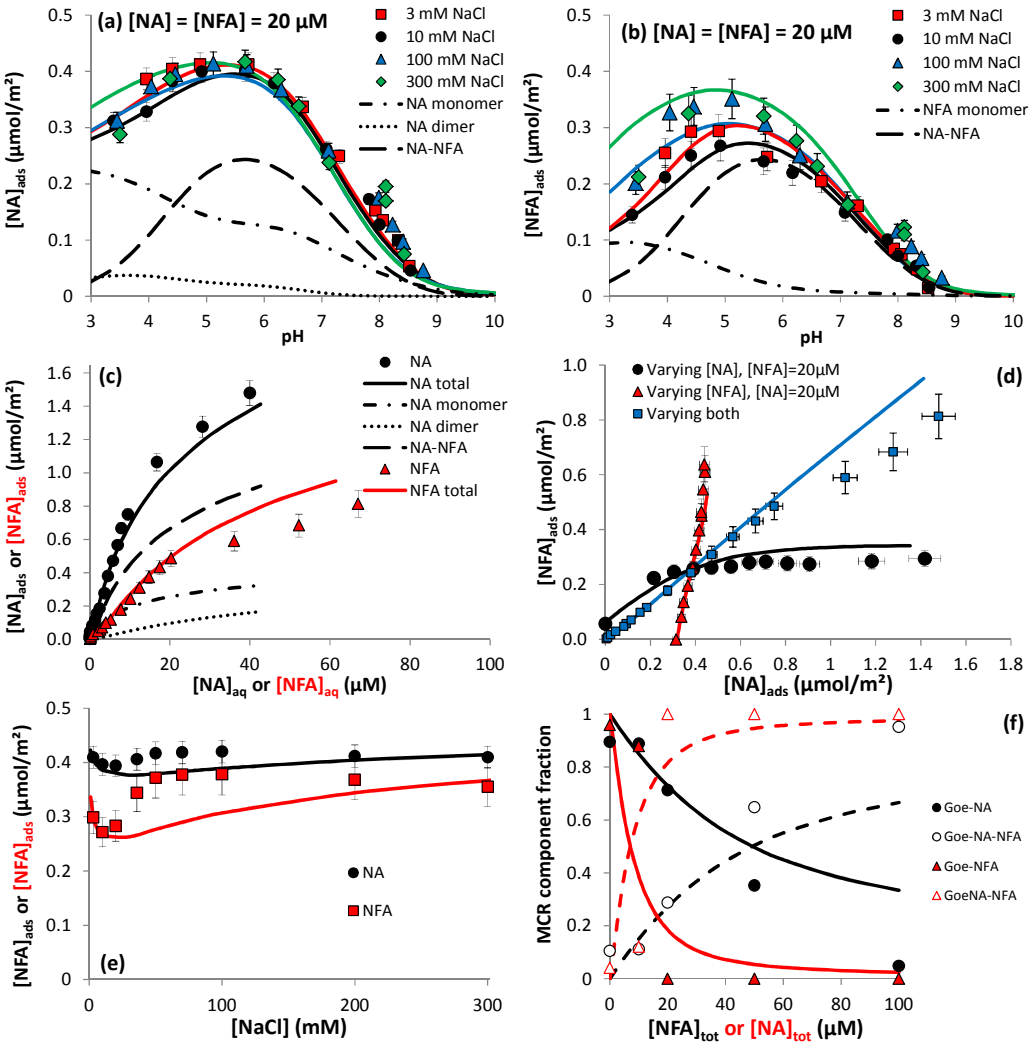
(a) [NA] = [NFA] = 20 µM
3 mM NaCl
10 mM NaCl
100 mM NaCl
300 mM NaCl
NA monomer
NA dimer
NA-NFA
[NA]ads (µmol/m²)
pH
(b) [NA] = [NFA] = 20 µM
NFA monomer
[NFA]ads (µmol/m²)
(c)
NA
NA total
NA monomer
NA dimer
NA-NFA
NFA
NFA total
[NA]ads or [NFA]ads (µmol/m²)
[NA]aq or [NFA]aq (µM)
(d)
Varying [NA], [NFA]=20µM
Varying [NFA], [NA]=20µM
Varying both
[NA]ads (µmol/m²)
(e)
[NaCl] (mM)
(f)
MCR component fraction
Goe-NA
Goe-NA-NFA
Goe-NFA
GoeNA-NFA
[NFA]tot or [NA]tot (µM)

**Figure 2**

562

TOC

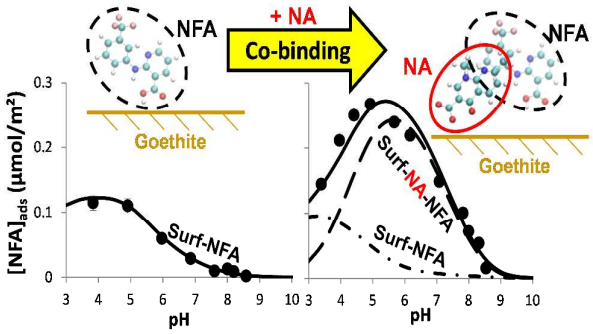
NFA
+ NA
Co-binding
NA
NFA
Goethite
Goethite
Surf-NFA
Surf-NA-NFA
Surf-NFA
[NFA]ads (µmol/m²)
0.3
0.2
0.1
0
3 4 5 6 7 8 9 10
pH
3 4 5 6 7 8 9 10
pH

563